Use of light scattering in characterizing reactively ion etched profiles

Konstantinos P. Giapis, Richard A. Gottscho,[a] Linda A. Clark, Joseph B. Kruskal, and Diane Lambert
AT&T Bell Laboratories, Murray Hill, New Jersey 07974

Avi Kornblit and Dino Sinatore
AT&T Bell Laboratories, Allentown, Pennsylvania 18103

(Received 29 October 1990; accepted 3 December 1990)

Currently, profile control in plasma etching of submicron structures requires inspection of cleaved samples by scanning electron microscopy. This is time consuming, destructive, and limited to a small subset of processed wafers. We show that light scattering can be used to rapidly characterize submicron differences in reactively ion etched, periodic Si structures. A similar approach has been used previously to monitor etching rates and undercutting using specular and first order diffraction peaks. Here, we measure all orders scattered over 180° as a function of incident angle and polarization and focus on the use of this technique coupled with statistical methodology to distinguish subtle changes in line profile. Although scatter from grating test patterns is examined here, this method should also be applicable to complex, submicron device structures.

I. INTRODUCTION

Common practice in the manufacturing of integrated circuits is periodic inspection of wafers for changes in critical dimension (linewidth), line shape, and etched depths. Previously, such inspections were performed nondestructively and rapidly using optical microscopy. With today's submicron patterns, however, selected wafers from a processing lot must be cleaved and inspected using scanning electron microscopy. This approach is obviously time consuming, destructive, and limited to a small subset of the wafer lot.

Light scattering from diffraction grating test patterns has been used previously to monitor etching rate during both wet and dry processes.[1–8] The first order relative to zeroth order (specular) intensity can be monitored in real time and related directly to etching rate. For wet processes, undercutting of the mask can be detected by loss of the first order diffracted light intensity.[1]

More recently, light scattering has been used for monitoring surface roughness after sputter deposition of metal films.[9–11] Rougher surfaces generate more diffuse, scattered light. In the same experimental arrangement, McNeil and co-workers have measured latent images of diffraction gratings in photoresist and hope to use this method for controlling exposure and development processes.[12] Grimard *et al.*[13] have recently reported measurements from relatively large but nonperiodic structures and have shown that the diffraction pattern is sensitive to gross changes in profile, from rectangular to trapezoidal.

In this work we report scattered light intensity as a function of diffraction angle, incident angle, and incident polarization for gratings in single crystalline Si formed by reactive ion etching. Scattered light intensity is plotted as a function of spatial frequency which is related to diffraction angle by

$$f=\frac{1}{d}=\frac{(\sin\theta_s-\sin\theta_i)}{\lambda},$$

where f is the spatial frequency in μm^{-1}, d is the grating period in μm, θ_s and θ_i are the scattered and incident angles, respectively, and λ is the wavelength in μm.

In general, there is a reciprocal relationship between the physical structure of the grating and the intensity modulation of the diffraction pattern. For example, the highest frequency oscillations in the diffraction pattern are primarily determined by the overlap of the incident laser beam and the diffraction grating. The lowest frequency oscillations in the diffraction pattern correspond to high frequency features such as anisotropically etched side walls. We do not attempt to resolve the finest structure in the diffraction pattern, but instead, take advantage of the reciprocal relationship and use large pitch, 32 μm, gratings to generate many harmonics in the diffraction pattern. Subtle changes in line shape for equal etch depths are then easily detected from changes in the intensity envelope.

Uniqueness is critical for this analytical technique. Can we distinguish two different profiles with equally etched depths from two identical profiles with unequally etched depths? Because only scattered light intensity is recorded and phase information is lost, uniqueness is not guaranteed and reconstruction of etched profiles is not possible. However, we show that diffraction intensity envelopes also depend on incident angle and polarization and with these additional independent variables, differentiation of structures appears both feasible and reliable. Diffraction patterns for processed structures can be cataloged and deviations from the norm easily detected. Thus, each wafer can be inspected rapidly and nondestructively.

II. EXPERIMENTAL DETAILS

Single crystalline Si wafers (125 mm diam) are patterned with grating test patterns using conventional photolithography. For nominally vertical or anisotropic profiles, the pat-

 0734-2101/91/030664-05$01.00

tern is transferred into a 7500 Å thick SiO_2 film that is the Si reactive ion etch (RIE) mask. For overcut profiles, a mask consisting of both photoresist (1.1 μm) and SiO_2 is used; simultaneous etching of the resist and the Si leads to the overcut profile. All etches are done in an Applied Materials Precision 5000 Etcher with Cl_2, SF_6, and He at 20 mTorr (2.66 Pa). A magnetic field of 100 G is rotated at a frequency of 2.2 Hz parallel to the wafer platen surface. Wafers are clamped and cooled using He gas on the backside to maintain a constant temperature of ~25 °C. Using a scanning electron microscope (SEM), linewidths after etching are measured to be 1.5 μm for overcut (near the mask) and vertical profiles. Undercut profile shapes depend on etch depth.

A variety of diffraction patterns with different periods are fabricated. Gratings with periods smaller than 32 μm gave qualitatively similar results to those shown here but since fewer orders are detected the envelope function is not so clearly defined and these patterns are not deemed as useful. Similarly, we also examined double, triple, and chirped period gratings but found no advantage in using such patterns. Although the grating area used here is 1.0×1.5 cm, the laser beam spot size is only ~0.08 cm^2 and much smaller areas could be used on real device wafers.

The monitoring setup is similar to that reported in Ref. 9. A HeNe laser (unfocused) is incident on the Si wafer at a polar angle (i.e., axis of rotation parallel to grooves) of either 0° ("normal") or 85.5°. For normal incidence, the laser is actually off-normal azimuthally, i.e., the wafer is rotated slightly about an axis perpendicular to the grooves; thus, diffraction is not in the incident plane and the specular beam is sampled without blocking the incident beam. As noted, a linear polarizer is sometimes placed at the output of the laser beam to sample either *s* or *p* polarization components; otherwise, the laser beam is unpolarized. Scattered light is detected at a constant radius (~20 cm) from the point of intersection between the laser beam and the wafer. A photodiode (Centronic OSD1-5B) with a "bugeye" lens (5 mm diam) is mounted on a computer-controlled rotary stage whose axis of rotation passes through the laser-beam-wafer intersection point. Angular resolution is ~0.012 rad; but as mentioned above, this is not critical as we are mostly interested in the lowest frequency intensity envelope. The laser beam is chopped and a phase-sensitive amplifier is used to discriminate scattered laser light from background sources of radiation. The amplifier output is sampled by an analog-to-digital converter and stored in the computer for subsequent display and analysis.

III. RESULTS AND DISCUSSION

In this study we are primarily concerned with determining how to use the diffraction intensity envelope to characterize line profiles. As shown in Fig. 1, diffraction patterns from two profiles etched to the same depth (1.5 μm) are easily distinguished. Although the etched profiles differ only on a submicron scale, differences in intensity envelopes are dramatic. For normal incidence, scattered light intensity from the "overcut" [Fig. 1(b)] profile is much stronger than from the "vertical" [Fig. 1(a)] profile. This seems reasonable since scattering from the sidewalls should be less important for the vertical profile. At grazing incidence, total scattered intensity is less affected by differences in sidewall profile but the intensity envelopes clearly show that the profiles can be distinguished. Polarization could also be exploited in providing differentiation between etched profiles as shown in Fig. 2. This added information may be redundant but useful for providing higher level confidence in the inspection process.

We also examined diffraction patterns from samples with similar profiles but which had been etched to different

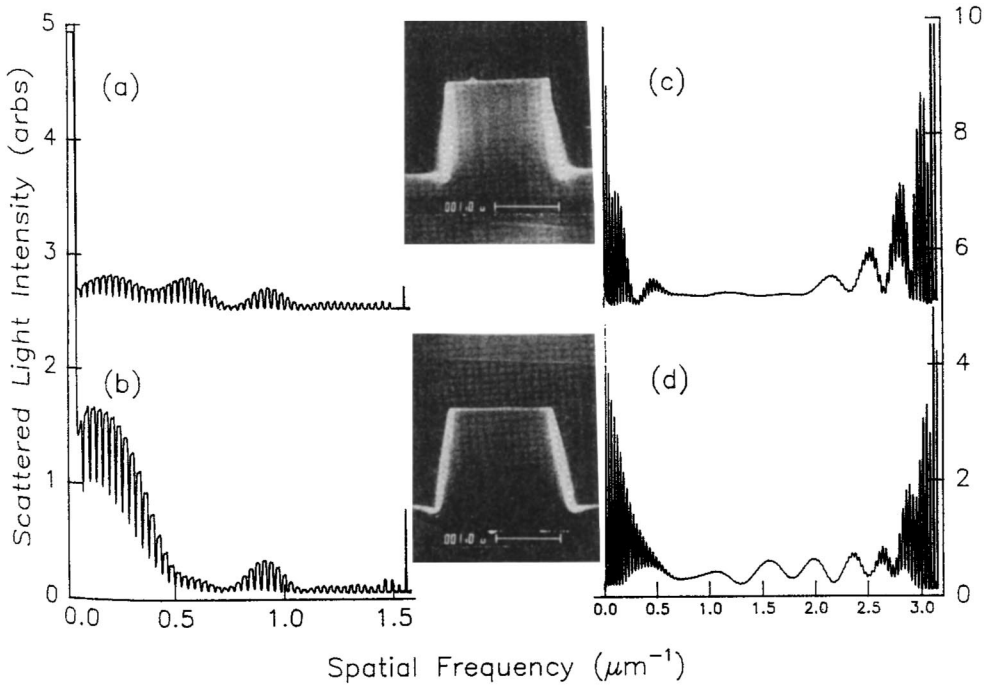

FIG. 1. Diffraction patterns from 32 μm period gratings etched into single crystalline Si. For (a) and (c) the profiles are nominally "vertical" as shown in the scanning electron microscope insert. For (b) and (d), the profiles are nominally "overcut." Both profiles are etched to the same depth. Normal (a) and (b) and grazing (c) and (d) incidence patterns are shown. The peaks correspond to harmonics of the fundamental spatial frequency of 0.031 25 μm^{-1}; the intensity envelope is dictated by the line shape and etched depth. In (a) and (c) the base line is shifted by 2.5 and 5.0, respectively.

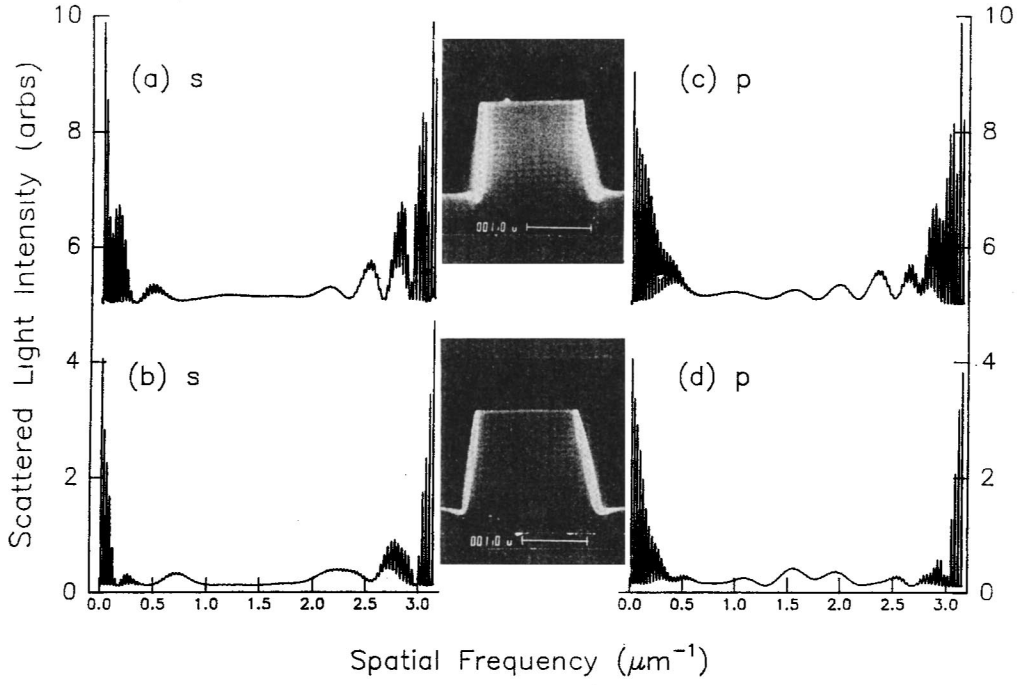

FIG. 2. Same as Fig. 1 except grazing incidence data are resolved into *s* and *p* polarization components. In (a) and (c) the base line is shifted by 5.0.

depths (Fig. 3). Regardless of incident angle, the patterns corresponding to different depths are distinct from one another and from the deeper etches with different profiles shown in Fig. 1. Here, the results are less intuitive and point out the need for further analysis and modeling. One naively expects more intense scattering from deeper profiles. This is observed at grazing incidence; but, at normal incidence, the scattered intensities are comparable.

These results are encouraging and suggest that light scattering could be used for rapid, postprocess inspection. To evaluate the feasibility of such an automated inspection procedure we developed a numerical procedure to catalog the data and determine significant deviations from a desired norm. Data sets corresponding to different masks, profiles, and depths were examined by:

(1) Removing the specular peak at 0° and then determining the envelope function by selecting the highest point of each diffraction peak. This is done by choosing each local maximum, defined as a value $\geqslant$ the four values on each side of it. Each envelope function then contains from 47 to 52 points.

(2) Linearly interpolating the envelope of each data set at 40 equally spaced spatial frequencies from 0.05 to 1.5. In some data sets, extrapolation is needed at the low end of the

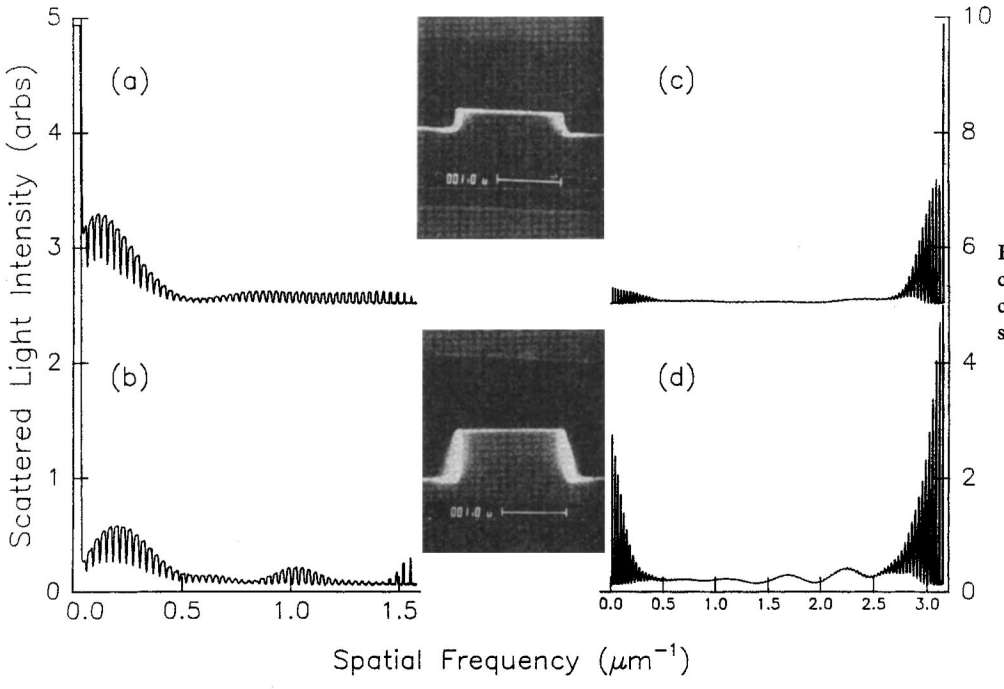

FIG. 3. Same as Fig. 1 except two "vertical" profiles etched to different depths are contrasted. In (a) and (c) the base line is shifted by 2.5 and 5.0, respectively.

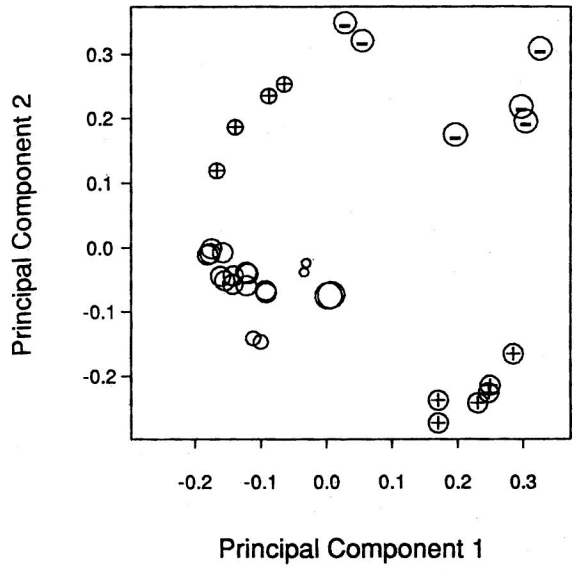

FIG. 4. First and second principal components from diffraction envelopes of 35 etched profiles in Si after stripping the mask. All data are for normal incidence. The area of the circle is proportional to etched depth with the largest circle corresponding to 2.8 μm and the smallest circle to 0.3 μm. Undercut and overcut profile data are symbolized by $-$ and $+$, respectively; vertical profiles correspond to empty circles. The vertical profiles bounded by $c1 = [-0.2, -0.10]$ and $c2 = [-0.1, 0.0]$ and the overcut profiles bounded by $c1 = [0.15, 0.30]$ and $c2 = [-0.3, -0.15]$ are etched to the same depth of 1.5 μm and are easily differentiated. The variation within these groups results from real variation in profiles at different positions on the chip (Fig. 5).

range. Put the interpolated values for the N data sets of interest into an $N \times 40$ matrix X. For Fig. 4, where the mask was stripped prior to analysis, $N = 35$.

(3) Analyzing X by the statistical method of "principal components analysis" (see, for example, Ref. 14). Principal components analysis produces a new orthogonal basis (the components) in which the first component accounts for most of the variation in the data and subsequent components are ordered by the amount of variation they account for. For our data sets, the coordinates with respect to the first two components provide an easily interpreted diagram, and the coordinates with respect to subsequent components are difficult to interpret.

Using this method the coordinates with respect to the first two principal components are determined and plotted as shown in Fig. 4. Note that for the same profile, etched depths are not all equal. Nonetheless, the method easily distinguishes between vertical and overcut profiles etched to the same or different depths. Although the undercut profiles are also clearly differentiated, it is currently unclear whether these differences result from differences in etched depth or profile. Within the vertical profile data, the same analysis can be performed and etch depth variation more clearly differentiated.

For equal depth and profile, the scatter evident in Fig. 4 results mostly from systematic variations in the diffraction pattern when the wafer is translated to examine different regions on the same chip. An example of such variation is shown in Figs. 5(a) and 5(b), where both diffraction patterns and SEM cross sections are shown for undercut profiles toward the wafer edge and center, respectively. Vari-

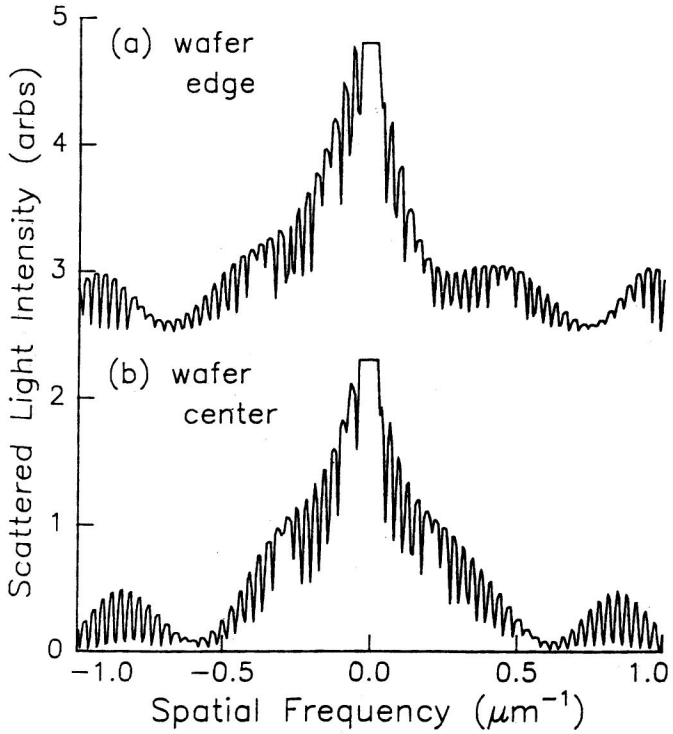

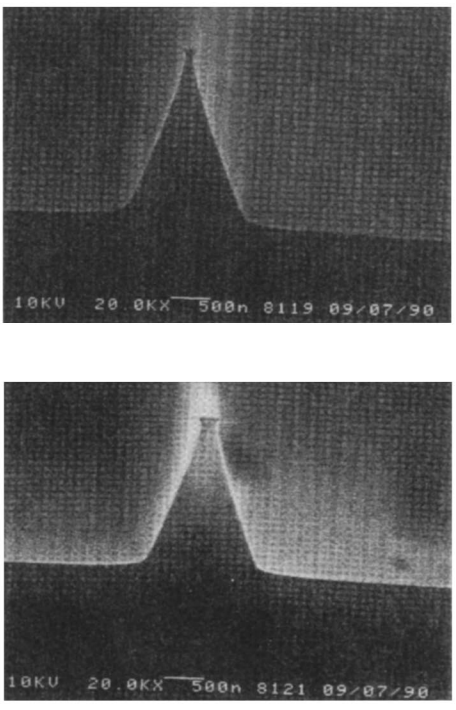

FIG. 5. Undercut diffraction patterns at normal incidence and SEM cross sections near wafer (a) edge and (b) center. The asymmetry in the diffraction pattern from negative to positive spatial frequencies is attributed to the laser beam size ($\sim$3 mm) being large compared to the distance over which the etched profile changes on the chip. Note that only a portion of the spatial frequency domain is plotted and the specular peak is off scale. The base line in (a) is offset by 2.5.

ation in etching depth and shape near the wafer edge is attributed to the proximity of fully masked area. Thus, reactant loading and ion bombardment are not the same on the edge as they are on the center. If the same position on the chip is examined repeatedly, either on the same wafer or on an identically etched wafer, the scatter is much reduced.

IV. CONCLUSION

Light scattering combined with the statistical methodology described provides a useful alternative to cleave and SEM inspection for statistical process control. Even with the scatter resulting from systematic variations in profile across the chip, deviations are readily detected. By setting limits on the first and second principal component values, for example, $[-0.2, -0.05]$ and $[-0.1, 0.0]$, respectively in Fig. 4, deviations from a 1.5 μm vertical etch are readily detected.

It should be noted that this method should apply to submicron device patterns; test patterns should not be necessary. However, if patterns are examined directly, alignment of the probe beam with respect to the device pattern will be crucial. It may also be necessary to use shorter wavelength light in this case to obtain sufficient envelope information. Work continues along these lines both to refine the experimental method and to determine the limits on etched depth and profile variation that can be reliably determined.

ACKNOWLEDGMENTS

We are grateful to J. R. McNeil, S. J. Brueck, T. Jewell, J. Jewell, and S. McCall for stimulating discussions on the subjects of scatterometry and diffraction theory.

[a] Author to whom correspondence should be addressed.

[1] H. P. Kleinknecht and H. Meier, J. Electrochem. Soc. **125**, 798 (1978).
[2] H. P. Kleinknecht and H. Meier, Appl. Opt. **19**, 525 (1980).
[3] H. P. Kleinknecht, Inst. Phys. Conf. Ser. No. **69**, 29 (1984).
[4] E. S. Braga, G. F. Mendes, J. Frejlich, and A. P. Mammana, Thin Solid Films **109**, 363 (1983).
[5] G. F. Mendes, L. Cescato, and J. Frejlich, Appl. Opt. **23**, 571 (1984).
[6] G. F. Mendes, L. Cescato, and J. Frejlich, Appl. Opt. **23**, 576 (1984).
[7] G. F. Mendes, L. Cescato, J. Frejlich, E. S. Braga, and A. P. Mammana, Thin Solid Films **117**, 107 (1984).
[8] G. F. Mendes, L. Cescato, J. Frjlich, E. S. Braga, and A. P. Mammana, J. Electrochem. Soc. **132**, 190 (1985).
[9] J. R. McNeil, L. J. Wei, G. A. Al-Jumaily, S. Shakir, and J. K. McIver, Appl. Opt. **24**, 480 (1985).
[10] G. A. Al-Jumaily, S. R. Wilson, and J. R. McNeil, SPIE **675**, 14 (1986).
[11] G. A. Al-Jumaily, S. R. Wilson, L. L. DeHainaut, J. J. McNally, and J. R. McNeil, J. Vac. Sci. Technol. A **5**, 1909 (1987).
[12] K. C. Hickman, S. M. Gaspar, K. P. Bishop, S. S. H. Naqvi, J. R. McNeil, G. D. Tipton, B. R. Stallard, and B. L. Draper, SPIE Microlithography Conference, March 5, 1991, San Jose, CA.
[13] D. S. Grimard, F. L. Terry, Jr., and M. E. Elta, Proc. SPIE **1185**, 234 (1990).
[14] J. B. Kruskal, in *International Encyclopedia of Statistics*, edited by W. H. Kruskal and J. M. Tanur (Macmillan, New York, 1978), pp. 307–330.